International Journal of Environmental Science and Technology (2023) 20:13191–13198
https://doi.org/10.1007/s13762-023-04866-0

ORIGINAL PAPER

A rapid colorimetric method for the determination of lead (II) at low concentrations in aqueous solution

A. Netzahual-Lopantzi[1] · L. Juárez-Santacruz[1] · E. García-Nieto[1]

Received: 1 February 2022 / Revised: 17 June 2022 / Accepted: 22 February 2023 / Published online: 6 March 2023

Abstract

Heavy metals like lead are highly toxic to human health and the environment. In this work we report a simple, reproducible and low-cost method to obtain a colorimetric nanosensor that selectively detects lead II in aqueous medium. The sensor is based on silver nanoparticles functionalized with 2-mercaptoethanol. Metallic nanostructures were obtained by the chemical reduction method. The X-ray diffraction spectra showed the face-centered cubic structure of the silver nanoparticles. The size of the crystallite was found to be 10 nm using Scherrer's equation. The colorimetric method takes advantage of the localized surface plasmon resonance properties of the metallic nanoparticles. Under alkaline conditions, mercaptoethanol helped to selectively detect Pb^{2+} over other metals, including As^{3+}, Cd^{2+}, Mg^{2+}, Fe^{3+} Ca^{2+}, and Na^{+} y K^{+}. A color change from yellow to bluish was recorded in the sensor when were mixed with lead ions. The experimental conditions allow carried out precipitation process in 8 min. On the other hand, the absorption spectra of lead samples were obtained by UV–Vis spectrometry to determine the detectable range of lead concentration, which was 0.04 µg/ml.

Keywords Mercaptoethanol · Lead II · Silver nanoparticles

Abbreviations

ME	2- Mercaptoethanol
AgNPs	Silver nanoparticles
LSRP	Localized surface plasmon resonance
UV	Ultraviolet
Vis	Visible
WHO	World Health Organization
EPA	Environmental protection agency
AAS	Atomic absorption spectroscopy
AFS	Atomic fluorescence spectrometry
ICP-MS	Inductively coupled plasma mass spectrometry
NPs	Nanoparticles
OH	Hydroxyl group
SH	Sulfhydryl group
COOH	Carboxyl group
NH_2	Amine group
LOD	Limit of detection
LOQ	Limit of quantification

Introduction

Environmental contamination by heavy metals is a topic of interest and great concern worldwide (López et al. 2020; Feitosa et al. 2021). Lead is among the most dangerous metals, since due to its chemical nature it represents a risk to human health and the environment (López et al. 2020). Although the origin of heavy metals may be natural, the high concentration in ecosystems is due to anthropic emissions (mining, agriculture and industry), which represents a risk of contamination. Lead (II) has been used in paints, gasoline, solder, plumbing, enamel, and many other applications. (Bratovcic 2020). Therefore, its distribution in the environment is wide. Studies published decades ago and recently demonstrated the wide distribution of lead. The heavy metals have been found in agricultural soils (Tian et al. 2022), in shooting ranges (Christou et al. 2022), sediments (Wakida et al. 2008), foods (Ortiz et al. 2017), springs or well water (Nieto et al. 2014) and rivers (López et al. 2020). In aqueous systems, lead exists predominantly in its divalent oxidation state (Pb^{2+}) (Feitosa et al. 2021). A small amount of Pb^{2+}

Editorial responsibility: Samareh Mirkia.

✉ A. Netzahual-Lopantzi
angelnetzahual@gmail.com

[1] Centro de Investigación en Genética Y Ambiente-Universidad Autónoma de Tlaxcala (CIGyA), Autopista San Martín-Tlaxcala Km 10.5, 90120 Ixtacuixtla, Tlaxcala, México

can cause damage to microorganisms (Wan et al. 2022) as well as to human health (Ortiz et al. 2017). It is highly toxic to the human body, having a negative impact on the kidneys (Chen et al. 2019), also associated with cardiovascular diseases. It even alters the expression of microRNA specifically miR-155 (Martinez et al. 2021).

According to World Health Organization (WHO) and Environmental Protection Agency (EPA, USA), the maximum permissible concentration of lead for, agricultural irrigation water is 2–5 µg/ml, for livestock consumption it is 0.1 µg/ml, water quality guidelines for recreational purposes is around 0.05 µg/ml and drinking water 0.015 µg/ml. Therefore, its detection with the naked eye is of vital importance. Several methods for the analysis of heavy metal ions have been developed in recent decades, including techniques based on atomic absorption spectroscopy (AAS), atomic fluorescence spectrometry (AFS), inductively coupled plasma mass spectrometry (ICP-MS) in various aqueous samples including drinking water, saltwater, lakes, etc. (Güzel et al. 2021). Although the aforementioned methods offer excellent sensitivity and multi-element analysis, they are expensive, time-consuming, skill-intensive, and laboratory-intensive, making it necessary to suggest alternative detection methods. Colorimetric methods based on Cu, Au and Ag nanoparticles (CuNPs, AuNPs and AgNPs) for the detection and quantification of heavy metals have gained importance in recent years (Sengan and Veerappan 2019; Sonia and Seth 2020; Boruah et al. 2019) due to the detection sensitivity, low cost without the need for a sophisticated laboratory. The principle of this colorimetric technique is the aggregation of NPs in the presence of heavy metals, changing the color of the original nanoparticles. Metallic nanostructures possess the optical property of localized surface plasmon resonance (LSPR), which allows obtaining precise quantitative information on the target molecules (Prosposito et al. 2019). In addition, with the NP-based method, results are obtained quickly, efficiently, economically and with high reproducibility.

Copper nanostructures functionalized with N-myristoyltaurine were used to detect mercury ions Hg^{2+}, the detection limit was 15 µM with the naked eye and by means of UV–Vis spectroscopy a limit of 0.1125 15 µM was recorded (Sengan and Veerappan 2019). Spherical Au nanoparticles ~ 30 nm conjugated with L-cysteine were prepared to detect concentrations of 10–40 ppm of cadmium in aqueous solutions (Sonia and Seth 2020). Nanometer-scale structures of silver functionalized with polyethylene glycol were used to specifically detect the arsenic ion III (Boruah et al. 2019). The nanosystem achieved a found detection limit of 1 ppb. It is important to mention that the colorimetric method uses functionalizing agents that help increase selectivity for heavy metals (Hyder et al. 2022). In this work, 2-mercaptoethanol (ME) was used to selectively detect lead ions at low concentrations. The ME linker is a short-chain molecule that has an –OH terminal at one end and a –SH at the other (Hong and Li 2013). It is well known that sulfhydryl functional groups bind to the surface of silver nanoparticles (Ramasamy et al. 2012). On the other hand, hydroxyls provide intermolecular binding forces to target molecules. The short length of ME ensures chemical and electromagnetic enhancements that amplify the optical transduction properties. The short length of ME ensures chemical and electromagnetic enhancements that amplify optical transduction, recorded either by UV–Vis or Raman spectroscopy (Hong and Li 2013; Filgueiras et al. 2016).

In this work, we present a new naked-eye colorimetric detection assay for the detection of Pb^{2+} in solution at low concentrations. AgNPs functionalized with 2-mercaptoethanol were used, which allowed observing the color change with the naked eye without the need for complex instrumentation.

Materials and methods

Materials

Silver nitrate $AgNO_3$, sodium citrate dihydrate ($Na_3C_6H_5O_7 \cdot 2H_2O$) purchased from J. T. Baker. Sodium borohydride ($NaBH_4 \geq 98.5\%$), 2-mercaptoethanol ($C_2H_6OS \geq 98\%$) and hydrochloric acid (NCl) acquired from Sigma-Aldrich. The test metal salts are listed below; lead nitrate ($PbNO_3$), calcium chloride dihydrate ($CaCl_2 \cdot 2H_2O$), sodium chloride (NaCl) and potassium chloride (KCl) were purchased from J. T. Baker. Cadmium chloride pentahydrate ($CdCl_2 \cdot 5H_2O$) obtained of Sigma. A standard arsenic solution was used (1 mg/ml) from Baker. Finally, magnesium chloride hexahydrate ($MgCl_2 \cdot 6H_2O$) and iron chloride hexahydrate ($FeCl_3 \cdot 6H_2O$) purchased from Merck. The reagents used did not need further purification. Deionized water from a Milli-Q (18.2 MΩcm) purification system was used in all aqueous solution preparations. Previously, the glassware vessels were cleaned with aqua regia solution, followed by a wash with deionized water.

Synthesis and functionalization of silver nanoparticles

The chemical reduction method was used to obtain silver nanoparticles according to Li et al. (2014) with slight modifications. Briefly, 250 µl of a solution silver nitrate (0.1 mol/L) was added to an Erlenmeyer flask containing 100 ml of deionized water at a temperature of ~ 5 ºC, the solution was mixed vigorously. Then, 1 ml of sodium citrate (0.1 mol/L) was added, 30 ml of fresh sodium borohydride solution (0.005 mol/L) was quickly poured into the

solution. The $NaBH_4$ reduces silver ions (Ag^+) to atomic silver (Ag°). In addition, sodium citrate stabilizes AgNPs. The color of the reaction solution changes from colorless to yellow, indicative of the formation of silver nanoparticles. The reaction mixture was allowed to stir for 30 min, and then the functionalization process was continued. Surface modification of AgNPs was performed in a one step. 1 ml of 2-ME linker solution (0.15 mmol/L) was added to 100 ml of colloidal solution. The resulting solution was mixed for a few seconds and used for heavy metal detection tests. The incubation of silver nanoparticles with metals was carried out at room temperature without the need for darkness.

Instrumentation

The colloidal solutions were characterized in a UV–Vis (spectrophotometer Jenway 6715, Fisher Scientific). A quartz cell with a path length of 10 mm was used. For X-ray diffraction (XRD) measurements, the Rigaku Smartlab diffractometer was used in Bragg–Brentano configuration, the samples were analyzed using CuKα radiation ($\lambda = 1.5418$ Å), the diffractometer was operated at a scanning speed of 0.02°/s in a 2θ range of 10–90°. The pH of the solutions was measured using a pH meter (model 2211 de Hanna, Instruments). The photograph was taken using high precision camera.

Results and discussion

Synthesis of silver nanoparticles

It is well known that silver nanoparticles have an absorption band in the visible region. In this case, the colloidal solution with mercaptoethanol presents a peak at 391 nm (shown in Fig. 1), which confirms the formation of nanoscale structures (Desai et al. 2012). Inset of Fig. 1 shows the yellow colloidal solution obtained.

On the other hand, the synthesized Ag nanoparticles were characterized by X-ray diffraction; the sample presented a typical XRD pattern as shown in Fig. 2. The crystal structure of the sample is well defined by the four sharp peaks at 2θ values of 38.5° (111), 44.7° (200), 65° (220) and 78.2° (311) related to the face cubic centered structure, according to Joint Committee on Powder Diffraction Standards (JCPDS card 04–0783) (Lange et al. 2010). The crystallite size D was estimated from the Debye–Scherer's equation, $D = \frac{0.9\lambda}{\beta * cos\theta}$ where $\lambda = 0.15414$ nm is the wavelength of the incident radiation, β is the full width at half maximum (FWHM) of the XRD peak (Lopantzi et al. 2022), in this case at 44.7°, finally θ is the Bragg angle. The D value was calculated around 10 nm.

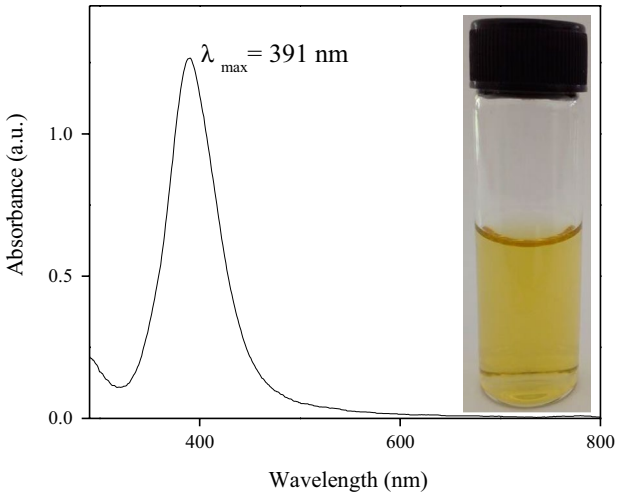

Fig. 1 UV–Vis spectrum of silver nanoparticles functionalized with 2-mercaptoethanol. *Inset*: colloidal solution obtained after the synthesis process

Selective colorimetric detection of lead (II)

Several heavy metal ions as well as other complementary metals (Pb^{2+}, As^{3+}, Cd^{2+}, Mg^{2+}, Fe^{3+} Ca^{2+}, and Na^+ y K^+) were taken for the selectivity test. In centrifuge tubes, concentrations of up to 5 µg/mL of heavy metals were mixed with newly synthesized functionalized AgNPs. The color change is evident in Fig. 3. It was observed that only the Pb^{2+} containing centrifuge tube shows a prominent color change to bluish while others are pale yellow. From this observation with the naked eye, the strong selectivity of functionalized silver nanoparticles toward lead (II) was evidenced.

The aforementioned samples were characterized by UV–Vis spectroscopy at room temperature. Figure 4a shows the spectra obtained. All the samples containing AgNPs-metals (less lead) presented slight modifications in the characteristic band of the silver nanoparticles. The colloidal sample containing lead II recorded a significant decrease in the peak at 391 nm. This effect is associated with the aggregation of silver nanoparticles in the presence of the heavy metal (Su et al. 2021). The influence of the degree of acidity-basicity on selectivity for heavy metals was investigated. Therefore, the pH of the colloidal solution was adjusted to 7.4 (native pH of the AgNPs solution is 9.5) using HCl at 1N. No significant changes could be recorded by UV–Vis spectroscopy, the band associated with SRPL was the same with or without heavy metal (shown in Fig. 4b). For our system, an alkaline pH (9.5) allowed to selectively recognize lead ions, similar results have been published previously (Xing et al. 2018). It is worth mentioning that non-functionalized silver nanoparticles (at pH 7.4 and 9.5) were mixed with heavy metals, but no affinity for lead was demonstrated (data not presented).

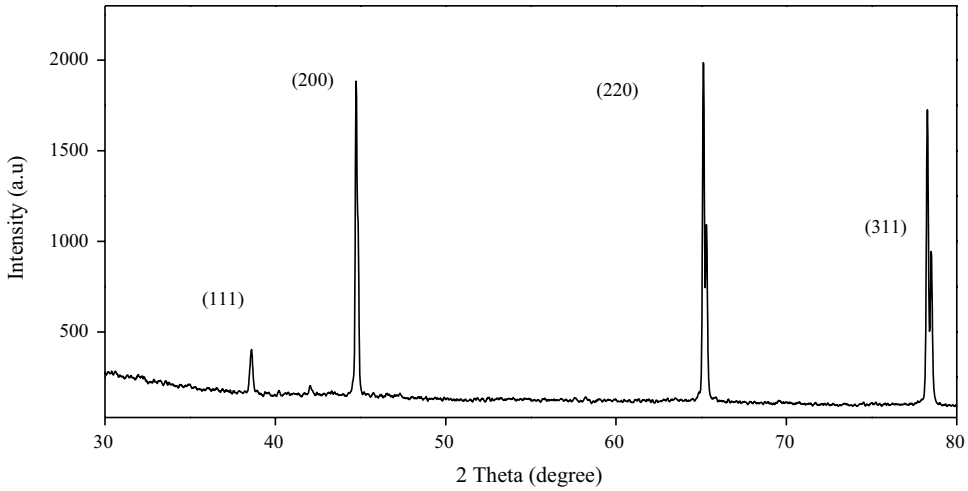

Fig. 2 XRD pattern of Ag particles synthesized from this work

Fig. 3 Photograph of centrifuge tubes containing heavy metal ions, where it is clarified that only the lead solution produces a color change in the original colloidal solution of AgNPs

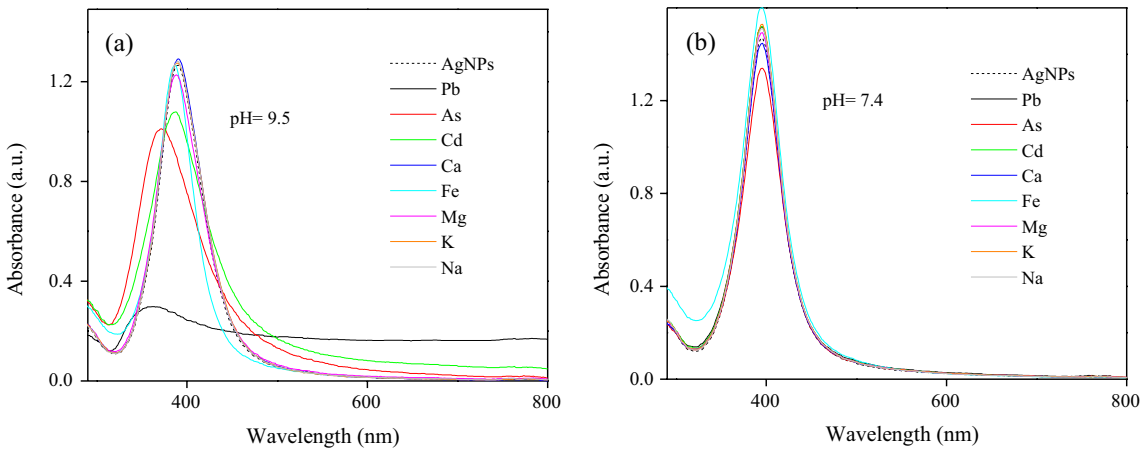

Fig. 4 UV–Vis spectra of the different test heavy metals mixed with solutions of silver nanoparticles at pH **a** alkaline 9.5 and **b** neutral 7.4

Mechanism of color change

A simple technique for the detection of lead (II) in aqueous medium using silver nanoparticles functionalized with 2-mercaptoethanol is reported here. Two crucial properties were used. First, the localized surface plasmon resonance of silver nanoparticles that depends on the dielectric constant of their surrounding environment. When the dielectric constant changes, the absorption peak shifts to longer wavelengths. Second, the short length of ME ~ 4 nm that ensures electromagnetic enhancement by amplifying the optical properties of transduction (Hong and Li 2013). The ME contains a sulfhydryl functional group –SH that binds to the surface of the silver and at the other end contains an –OH group (Ramasamy et al. 2012). The hydroxyl provides solubility and negative charges to the particle surface that prevents its aggregation due to electrostatic or steric repulsion (Xavier et al. 2014). When lead was introduced to these functionalized silver nanoparticles, it interacts with the hydroxyl groups. Due to this interaction, the aggregation of silver nanoparticles occurs. This means that the environment of the silver nanoparticles changes. Therefore, there is

a decrease in the peak at 391 nm and other bands appear at longer wavelengths. This effect produces a color change in the colloidal samples from yellow to bluish. Figure 5 shows the mechanism. Furthermore, we evaluated the selectivity of the colorimetric sensor at two different pH values. According to the results, we observe that at pH = 7.4 the AgNPs-ME do not precipitate in the presence of lead. From these observations, we suggest that, under neutral conditions, the hydroxyl does not completely deprotonate and avoid recognizing Pb^{2+} ions. The selectivity of –OH for heavy metal ions found here has also been reported with other functional groups with a negative nature such as carboxylic groups (–COOH) and amines ($–NH_2$) (Anambiga et al. 2013).

Reaction time on AgNPs-ME aggregation induced by Pb^{2+}

Absorption spectra were taken periodically (every 2 min) to estimate the reaction rate. Figure 6 shows the UV–Vis spectra taken from minute 0 to 14 and at concentration of 2 µg/ml of lead. A decrease in the intensity of the absorption peak of λ_{391} could be observed from the first seconds of incubation with the AgNPs-Pb^{2+}. The decrease in a LSPR band and formation of a shoulder at longer wavelengths was more evident with time. The spectra corresponding to minute 8, 10, 12, and 14 (pink, green, orange and gray spectrum of Fig. 6) have the same behavior. Which means that ME-functionalized AgNPs have a high affinity for lead ions. The reaction speed obtained in this work even exceeds other previously published works (Choudhury and Misra 2018).

Limit of detection and limit quantification

Limit of detection (LOD), linear range and limit of quantification (LOQ) were calculated because they are very important parameters in colorimetric sensors (Boruah et al. 2019). Various samples were evaluated at low Pb^{2+} concentrations to obtain the detectable range of lead II. For this, 1 ml of functionalized nanoparticles was mixed with

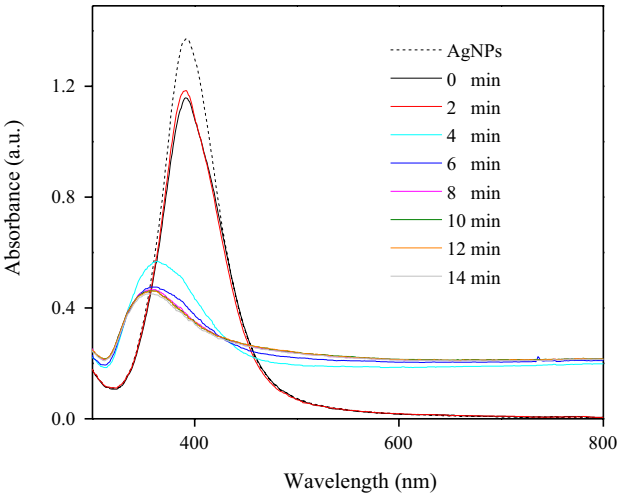

Fig. 6 **a** UV–Vis spectral behavior of AgNPs-Pb^{2+} (2 µg/ml) at different times

1 ml of deionized water containing 1–2 µg of Pb^{2+}. After 8 min of storage at room temperature, the different samples were characterized by UV–Vis in a range of 200 to 800 nm (shown in Fig. 7a). A decrease in the absorption peak of λ_{391} and the formation of a second band at higher wavelengths were recorded as the concentration of heavy metals increased. On the other hand, a deconvolution was also performed in the 300–750 nm region. Figure 7b shows the results obtained by mixing 2 µg/ml of lead with AgNPs. It was possible to observe the formation of three subbands located at 380, 415 and 520 nm (green line), the sum (red line) and the experimental spectra (black line). These three subbands were recorded in all samples containing Pb^{2+} ions, data not shown. The band located at 520 nm was associated with the aggregation of nanostructures (Choudhury and Misra 2018) and consequently was used in subsequent measurements.

Absorbance ratio values of $A_{520/391}$ were used to assess detection sensitivity in aqueous medium. The $A_{520/391}$ value of the lead-free AgNPs was found to be 0.0387. When AgNPs are in the presence of lead at 1 and 1.8 µg/ml, the

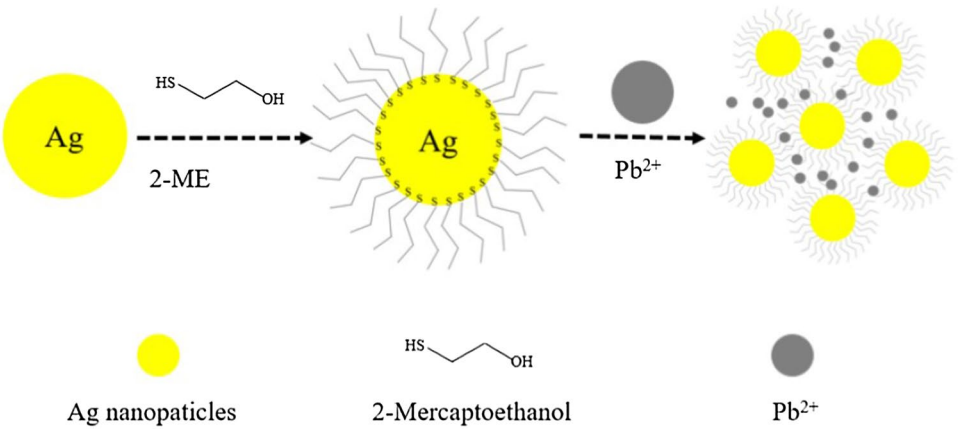

Fig. 5 Schematic representation of the proposed AgNPs-ME aggregation process in the presence of lead

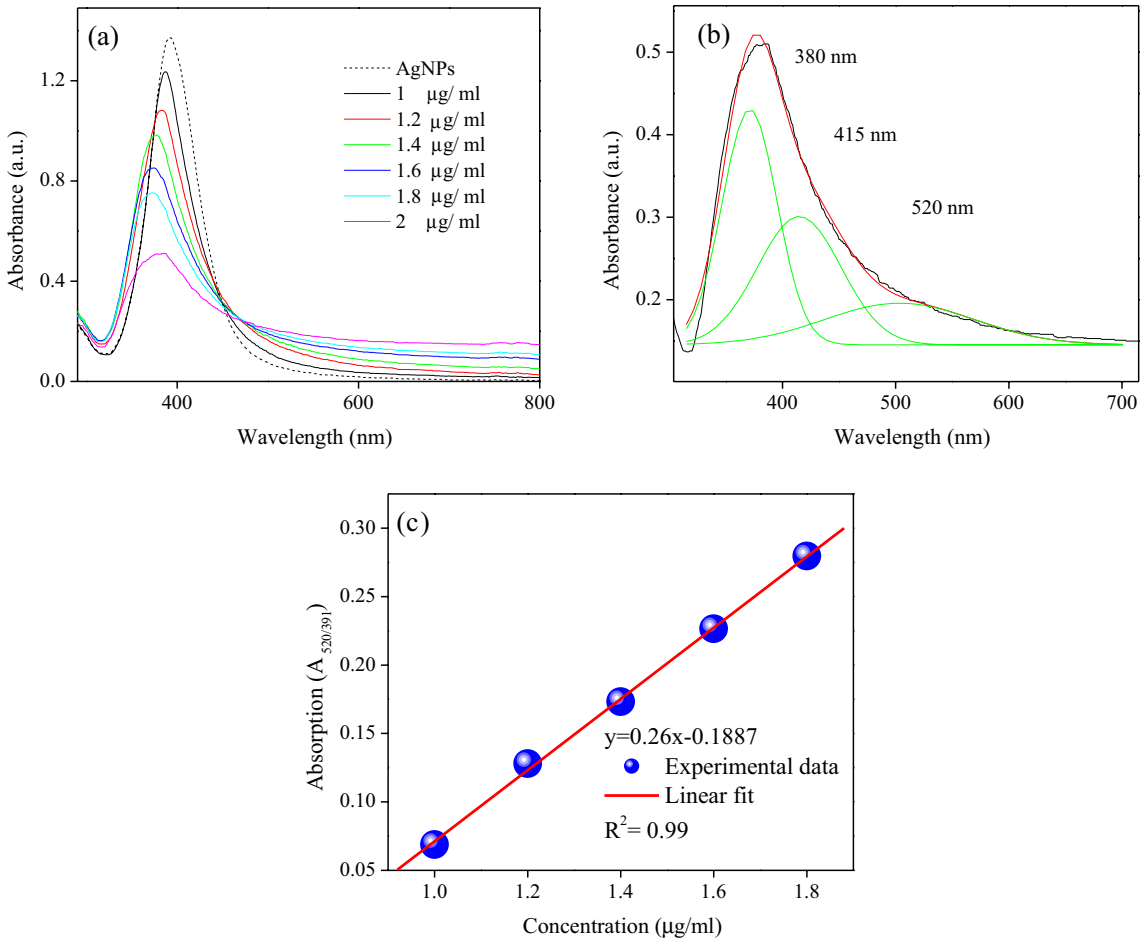

Fig. 7 **a** Absorption vs different concentrations of lead, **b** deconvolution of the spectrum of Pb^{2+}-AgNPs containing 2 µg/ml of the heavy metal and **c** linear response of colorimetric detection of A_{520}/A_{391} vs Pb^{2+} concentration

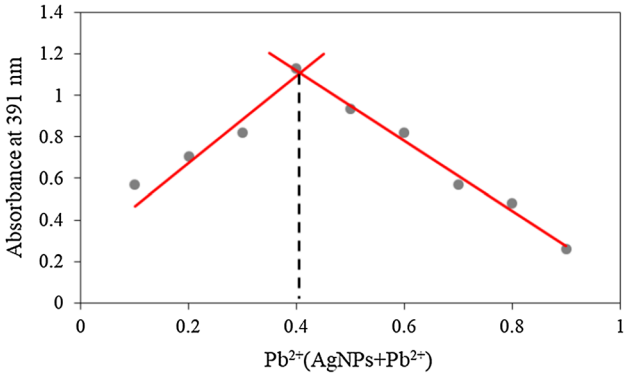

Fig. 8 Job plot determination for the binding stoichiometry between AgNP and Pb^{2+} monitored at 412 nm

ratio value increased to 0.0689 and 0.2796, respectively (shown in Fig. 7c). The aforementioned results helped to calculate the linear range. Figure 7c shows a linearity of relationship 520/391 depending on the concentration of lead. An $R^2 = 0.99$ was estimated between the values 1 and 1.8 µg/ml of lead, a slope of $m = 0.26$, with these data and the standard deviation σ it is possible to calculate the limit of detection (LOD) and the limit of quantification (LOQ) (Qi et al. 2012). The LOD y LOQ are obtained from the following relationship $3\sigma/m$ y $10\sigma/m$ being 0.04 and 0.12 µg/ml, respectively.

Jot-plot

To determine the union stoichiometry between Pb^{2+} and AgNP the Job graph was made (Fig. 8). Changes in absorbance at 391 nm were used for this estimation. In separate vials, 0.2, 0.4, 0.6, 0.8, 1, 1.2, 1.4, 1.6 and 1.8 ml of heavy metal solutions at 1 mM were taken. To these lead solutions 1.8, 1.6, 1.4, 1.2, 1, 0.8, 0.6, 0.4 and 0.2 ml of AgNPs solution were added, respectively, as that the total volume of the solution was 2 ml. A binding stoichiometry of 2:3 was found between AgNPs y Pb^{2+}, respectively. The results obtained here indicate that fewer moles of lead (II) are needed to precipitate silver particles compared to previous reports (Huang 1982; Wang and Zheng 2017).

Table 1 Comparison of colorimetric sensors based on silver nanoparticles to detect Pb^{2+}

Reagent	Synthesis method	Detection method	LOD	References
Iminodiacetic acid	2 h in the dark	Naked-eye & UV–vis spectroscopy	13 nM	Qi et al. (2012)
Glutathion	2 h in dark	Naked-eye & UV–vis spectroscopy	0.01 µM	Anambiga et al. (2013)
1-(2-mercaptoethyl)-1,3,5-triazinane-2,4,6-trione (MTT)	6 h under nitrogen atmosphere	Naked-eye & UV–vis spectroscopy	0.4 µg/ml	Noh et al. (2015)
3,4-dihydroxy-L-phenylalanine (DOPA)	3 h	Naked-eye & UV–vis spectroscopy	94 µM	Cheon and Park (2016)
Gluconate	30 min	Naked-eye & UV–vis spectroscopy	0.2 µM	Choudhury and Misra (2018)
Dithizone	1 h	Naked-eye & UV–vis spectroscopy	0.64 µg/L	Roto et al. (2019)
2-Mercaptoethanol	30 min	Naked-eye & UV–vis spectroscopy	0.04 µg/ml	This work

Here we report a simple, inexpensive, reproducible method without the need for expensive equipment to obtain a colorimetric sensor based on AgNPs-ME. The synthesis can be carried out under atmospheric conditions. Unlike to Noh et al. (2015), the authors synthesized an AgNPs nanosensor in the presence of nitrogen at 6 h of reaction. The selectivity of our system is high without the need for masking agents. Such as Hung et al. (2010) who detect Pb^{2+} ions with gold nanostructures functionalized with mercaptoethanol in the presence of sodium sulfide. The pH, reaction rate, binding stoichiometry, detection limits and quantification limit found in this work are comparable with others previously published. In this work, the high concentration tested was 5 µg/ml, so the nanosensor solution changed from yellow to bluish. It is worth mentioning that the colorimetric sensor developed here offers high sensitivity with a detected concentration of lead II at 0.04 µg/ml or 193 nM, lower values than other techniques such as voltammetric method reported by Huseinov et al. (2021). The authors used a platinum electrode to quantify Pb^{2+}, the reported detection limit was 34.5 µM heavy metal. Table 1 summarizes the LOD values reported by other authors using colorimetric sensors.

Conclusion

A simple and easy method was developed to obtain a colorimetric sensor based on silver nanoparticles (with a crystallite size of ~ 10 nm) functionalized with 2-mercaptoethanol. Under alkaline conditions, ME helped to selectively detect Pb^{2+} among other heavy metals, with a detection speed of 8 min. To the naked eye, the nanosensor changed color from yellow to bluish in the presence of high concentrations of lead, such as 5 µg/ml. On the other hand, the sensitivity of the nanosystem made it possible to detect lead at low concentrations of 0.04 µg/ml, without the need for a sophisticated laboratory, and by means of UV–Vis spectroscopy. The values found here were below the maximum allowed for aquatic systems. The binding stoichiometry was 2:3 AgNPs:Pb^{2+}, respectively. Therefore, compared to other spectroscopy methods, the colorimetric sensor developed here is competitive in terms of detection limit, simplicity, and convenience.

Acknowledgements Thanks to CONACYT (México) under scholarship No. 948409, to CIGyA and the Universidad Autónoma de Tlaxcala for supporting this work.

Declarations

Conflict of interest The authors declare no conflict of interest.

Ethical approval This article does not contain any studies with human participants or animals performed by any of the authors.

References

Anambiga LV, Suganthan V, Raj NAN, Buvaneswari G, Kumar TSS (2013) Colorimetric detection of lead ions using glutation stabilized silver nanoparticles. Int J Sci Eng Res 4:710–715

Boruah BS, Daimari NK, Biwas R (2019) Functionalized silver nanoparticles as an effective medium towards trace determination of arsenic (III) in aqueous solution. Results Phys 12:2061–2065. https://doi.org/10.1016/j.rinp.2019.02.044

Bratovcic A (2020) Synthesis, characterization, applications, and toxicity of lead oxide nanoparticles. Lead Chem Intechopen. https://doi.org/10.5772/intechopen.91362

Chen X, Zhu G, Wang Z, Zhou H, He P, Liu Y, Jin T (2019) The association between lead and cadmium co-exporuse and renal dysfunction. Ecotoxicol Environ Saf 173:429–435. https://doi.org/10.1016/j.ecoenv.2019.01.121

Cheon JY, Park WH (2016) Green synthesis of silver nanoparticles stabilized with mussel-inspired protein and colorimetric sensing of lead (II) and copper (II) ions. Int J Mol Sci 17:1–10. https://doi.org/10.3390/ijms17122006

Choudhury R, Misra TK (2018) Gluconate stabilized silver nanoparticles as a colorimetric sensor for Pb^{2+}. Colloids Surf A 545:179–187. https://doi.org/10.1016/j.colsurfa.2018.02.051

Christou A, Hadjisterkotis E, Dalias P, Demetriou E, Christofidou M, Kozakou S, Michael N, Charalambous C, Hatzigeorgiou M, Christou E, Stefani D, Christoforou E, Neocleous D (2022) Lead contamination of soils, sediments, and vegetation in a shooting range and adjacent terrestrial and aquatic ecosystems: A holistic approach for evaluating potential risks. Chemosphere 292:1–8. https://doi.org/10.1016/j.chemosphere.2021.133424

Desai R, Mankad V, Gupta SK, Jha PK (2012) Size distribution of silver nanoparticles UV-Visible spectroscopic assessment.

Nanosci Nanotechnol Lett 4:30–34. https://doi.org/10.1166/nnl.2012.1278

Feitosa MM, Alvarenga LFS, Jara MS, Lima GJEO, Vilela FJ, Resende T, Guilherme LRG (2021) Environmental and human-health risks of as in soils with abnormal arsenic levels located in irrigated agricultural areas of Paracatu (MG). Brazil Ecotoxicol Environ Safety 226:1–11. https://doi.org/10.1016/j.ecoenv.2021.112869

Filgueiras AL, Lima FR, de Carvalho DF, Meirelles MA, Paschoal D, dos Santos HF, Sanchez-Cortes S, Santana AC (2016) The adsorption of rifampicin on gold or silver surfaces mediated by 2-mercaptoetanol investigated by surface-enhanced Raman scattering spectroscopy. Vib Spectroscs 86:75–80. https://doi.org/10.1016/j.vibspec.2016.06.006

Güzel B, Canli O, Aslan E (2021) Spatial distribution, source identification and ecological risk assessment of POPs and heavy metals in lake sediments of Istambul. Turk Marine Pollut Bull 175:1–14. https://doi.org/10.1016/j.marpolbul.2021.113172

Hong S, Li X (2013) One-step surface modification of gold nanoparticles for surface-enhanced Raman spectroscopy. Appl Surf Sci 287:318–322. https://doi.org/10.1016/j.apsusc.2013.09.149

Huang C (1982) Determination of binding stoichiometry by the continuous variation method: the job plot. Methods Enzymol 87:509–525. https://doi.org/10.1016/S0076-6879(82)87029-8

Hung YL, Hsiung TM, Chen YY, Huang YF, Huang CC (2010) Colorimetric detection of heavy metal ions using label-free gold nanoparticles and alkanethiols. J Phys Chem C 114:16329–16334. https://doi.org/10.1021/jp1061573

Huseinov A, Weese BL, Brewer BJ, Alvarez NT (2021) Near-electrode pH change for voltammetric detection of insoluble lead carbonate. Anal Chim Acta 1186:1–7. https://doi.org/10.1016/j.aca.2021.339087

Hyder A, Buledi JA, Nawaz M, Rajpar DB, Shah ZH, Orooji Y, Yola ML, Maleh HK, Lin H (2022) Identification of heavy metal ions from aqueous environment through gold, silver and copper nanoparticles: an excellent colorimetric approach. Environ Res 205:1–11. https://doi.org/10.1016/j.envres.2021.112475

Lanje AS, Sharma SJ, Pode RB (2010) Synthesis of silver nanoparticles: a safer alternative to conventional antimicrobial and antibacterial agents. J Chem Pharm Res 2(3):478–483

Li Z, Wang Y, Ni Y, Kokot S (2014) Unmodified silver nanoparticles for rapid analysis of the organophosphorous pesticide, dipterex, often found in different waters. Sens Actuators, B Chem 193:205–2011. https://doi.org/10.1016/j.snb.2013.11.096

Lopantzi AN, Santacruz LJ, Nieto EG, Pérez JLJ, Ibarra ICR, Vidal UOG, Orea AC (2022) Study of the thermal diffusivity and optical properties of lead oxide nanoparticles annealed at different temperatures. Int J Thermophys 43(83):1–14. https://doi.org/10.1007/s10765-022-03013-0

López E, Patiño R, Sauceda MLV, Castañeda RP, Méndez LUA, Ventura R, Heyer L (2020) Water quality and ecological risk assessment of intermittent stramflow thorugh mining and urban áreas of San Marcos River sub-basin, Mexico. Environ Nanotechnol, Monit Manag 14:1–9. https://doi.org/10.1016/j.enmm.2020.100369

Martínez ACO, Silva JAV, García STO, Yáñez LC, Maldonado INP (2021) Lead (Pb) exporuse is associated with changes in the expression levels of circulating miRNAS (miR-155, miR-126) inMexican women. Environ Toxicol Pharmacol 83:1–7. https://doi.org/10.1016/j.etap.2021.103598

Nieto EG, Santacruz LJ, Gallegos EG, Zempoalteca JT, Gómez CR (2014) Genotoxical response of the common carp (*Cyprinus carpio*) exposed to spring water in Tlaxcala. Mexico Bull Environ Contam Toxicol 93:393–398. https://doi.org/10.1007/s00128-014-1318-2

Noh KC, Nam YS, Lee HJ, Lee KB (2015) A colorimetric probe to determine Pb^{2+} using silver nanoparticles. Analyst 140:1–22. https://doi.org/10.1039/C5AN01601K

Ortiz EO, Nieto EG, Santacruz LJ, Camarillo MAG, Gallegos EG, Huitrón PL (2017) Lead exporuse: pottery impact in Tlaxcala. Mexico Rev Int Contam Ambie 33:57–64. https://doi.org/10.20937/rica.2017.33.01.05

Prosposito P, Burratti L, Venditti I (2019) Silver nanoparticles as colorimetric sensors for water pollutants. Chemosensors 8:1–29. https://doi.org/10.3390/chemosensors8020026

Qi L, Shang Y, Wu F (2012) Colorimetric detection lead (II) based on silver nanoparticles capped with iminodiacetic acid. Microchim Acta 178:221–227. https://doi.org/10.1007/s00604-012-0832-3

Ramasamy P, Seo DM, Kim SH, Kim J (2012) Effects of TiO_2 on optical and thermal properties of silver nanowires. J Mater Chem 22:11651–11657. https://doi.org/10.1039/C2JM00010E

Roto R, Mellisani B, Kuncaka A, Mudasir M, Suratman A (2019) Colorimetric sensing Pb^{2+} ion by using Ag nanoparticles in the presence of dithizone. Chemosensors 7(28):1–12. https://doi.org/10.3390/chemosensors7030028

Sengan M, Veerappan A (2019) N-myristoyltaurine capped copper nanoparticles for selective colorimetric detection of Hg^{2+} in wastewater and as effective chemocatalyst for organic dye degradation. Microchem J 148:1–9. https://doi.org/10.1016/j.microc.2019.04.049

Sonia SR (2020) L-cysteine functionalized gold nanoparticles as a colorimetric sensor for ultrasensitive detection of toxic metal ion cadmium. Mater Today: Proc 24:2375–2382. https://doi.org/10.1016/j.matpr.2020.03.767

Su YC, Lin AY, Hu CC, Chiu TC (2021) Functionalized silver nanoparticles as colorimetric probes for sensing tricyclazole. Food Chem 347:1–7. https://doi.org/10.1016/j.foodchem.2021.129044

Tian K, Li M, Hu W, Fan Y, Huang B, Zhao Y (2022) Environmental capacity of heavy metals in intensive agricultural soils: Insights from geochemical baselines and source apportionment. Sci Total Environ 819:1–39. https://doi.org/10.1016/j.scitotenv.2022.153078

Wakida FT, Ruiz DL, Peña JT, Ventura JGR, Díaz C, Flores EG (2008) Heavy metals in sediments of the Tecate river Mexico. Environ Geol 54:637–642. https://doi.org/10.1007/s00254-007-0831-6

Wan Y, Devereux R, Geroge SE, Chen J, Gao B, Noerpel M, Scheckel K (2022) Interactive effects of bioachar amendment and lead toxicity on soil microbial community. J Hazard Mater 425:1–10. https://doi.org/10.1016/j.jhazmat.2021.127921

Wang D, Zheng XJ (2017) A colorimetric chemosensor for Cu (II) ion in aqueous medium. Inor Chem Com 84:178–181. https://doi.org/10.1016/j.inoche.2017.08.017

Xavier SSJ, Karthikeyan C, Kumar GG, Kim AR, Yoo DJ (2014) Colorimetric detection of melamine using B-cyclodextrin-functionalized silver nanoparticles. Anal Methods 6:8165–8172. https://doi.org/10.1039/C4AY01183J

Xing TY, Zhao J, Weng GJ, Li JJ, Zhu J, Zhao JW (2018) Synthesis of dual functional Ag/Au nanoparticles based on decreased cavitating rate under alkaline condition and the colorimetric detection of mercury (II) and lead (II). J Mater Chem C 6:7557–7567. https://doi.org/10.1039/C8TC01867G